Differences in shoulder belt fit for females versus males measured using upright open magnetic resonance imaging

Citation for the original published paper (version of record):
Mergler, O., Espelien, C., Booth, G. et al (2025). Differences in shoulder belt fit for females versus males measured using upright open magnetic resonance imaging. Journal of Biomechanics, 185. http://dx.doi.org/10.1016/j.jbiomech.2025.112676

Journal of Biomechanics 185 (2025) 112676

Contents lists available at ScienceDirect

Journal of Biomechanics

journal homepage: www.elsevier.com/locate/jbiomech

Differences in shoulder belt fit for females versus males measured using upright open magnetic resonance imaging

Olivia Mergler [a,*], Corina Espelien [a], Gabrielle R. Booth [b], Carolyn Roberts [b], Paris Vakiel [c], Sarah Romani [d], Honglin Zhang [c], Bengt Pipkorn [e], Gunter P. Siegmund [b,f], Peter A. Cripton [g], Jason Forman [a]

[a] Center for Applied Biomechanics, University of Virginia Center for Applied Biomechanics, 4040 Lewis and Clark Dr., Charlottesville, VA 22911, United States
[b] MEA Forensic Engineers & Scientists, 23281 Vista Grande Drive, Laguna Hills, CA 92653, United States
[c] University of British Columbia, 798 - 2635 Laurel Street, Vancouver, BC V5Z 1M9, Canada
[d] University of British Columbia, 2222 Health Sciences Lane, Vancouver, BC V6T 1Z3, Canada
[e] Autoliv Research and Chalmers University, Wallentinsvägen 22 Vargarda, Västergötland 44793, Sweden
[f] School of Kinesiology, University of British Columbia, 210-6081 University Boulevard, Vancouver, BC V6T 1Z1, Canada
[g] School of Biomedical Engineering, University of British Columbia, 2222 Health Sciences Mall, Vancouver, BC V6T 1Z3, Canada

ARTICLE INFO

Keywords:
Automotive
Seat belt
Restraint
Soft tissue
Imaging

ABSTRACT

In comparisons of similar crashes between sexes, females exhibit an elevated risk of injury to the cervical spine and ribs. This preliminary study aims to investigate the relationship between upper body shape and shoulder belt fit, which may provide further insight into sex-based differences in seat belt loading and potential injury patterns. A non-ferromagnetic seat was fabricated for use with an open magnetic resonance (MR) imaging system, as well as a seat belt made of standard automotive webbing material with MR-visible markers. MR scans were acquired for 10 volunteers (5 female, 5 male) in an upright self-selected seat back position. This analysis focused on the shoulder belt positioning relative to the sternum and clavicle, with consideration of soft tissue interactions on this routing. Females in this study exhibited over three times greater range in the distance of the shoulder belt to the top of the sternum (SBD) compared to the males, despite similar or less variability than males in all gross anthropometric measures (SBD range, females: 21–116 mm, males: 51–78 mm). Such differences in variability highlight the diversity in routing patterns that may be influenced by different body geometries, such as breast tissue volume and distribution. Understanding how shoulder belt fit varies among and within diverse occupant populations highlights the need for improving the robustness of restraint design and performance.

1. Introduction

Understanding human variability is critical to inform the interactions between vehicle occupants and restraint systems. Factors including age, overall body geometries, and sex have been widely explored to investigate risk factors associated with injury in automobile collisions. For example, increased fragility of the ribs that occurs during aging can be associated with a heightened risk of thoracic injury (e.g., rib fracture) in an automobile collision (Forman et al., 2019; Hanna and Hershman, 2009; Kent et al., 2005). Obesity, defined by a high body mass index (BMI), can be a critical factor for many injuries, including severe rib injury, due both to the greater occupant excursion in a collision and the change in restraint-to-body interaction from increased adipose tissue (Boulanger et al., 1992; Gepner et al., 2018). Females are at a higher risk for rib fractures and cervical spine injuries compared to males when controlling for other factors, like age and BMI (Forman et al., 2019), although that difference in risk may also be related to factors such as systematic differences in the size of vehicles that females and males drive (Brumbelow and Jermakian, 2022). Identifying how current safety equipment engages with the occupants may provide insight and context into observed differences in injury risk for females versus males and other diverse populations (Forman et al., 2019; Jones et al., 2018; Reed et al., 2013).

* Corresponding author.
E-mail addresses: orm2119@columbia.edu (O. Mergler), cme2kd@virginia.edu (C. Espelien), gabrielle.booth@meaforensic.com (G.R. Booth), carolyn.roberts@meaforensic.com (C. Roberts), paris.vakiel@ubc.ca (P. Vakiel), sarahromani@outlook.com (S. Romani), Honglin.Zhang@hiphealth.ca (H. Zhang), Bengt.Pipkorn@autoliv.com (B. Pipkorn), gunter.siegmund@meaforensic.com (G.P. Siegmund), peter.cripton@ubc.ca (P.A. Cripton), jlf3m@virginia.edu (J. Forman).

https://doi.org/10.1016/j.jbiomech.2025.112676
Accepted 1 April 2025
Available online 4 April 2025

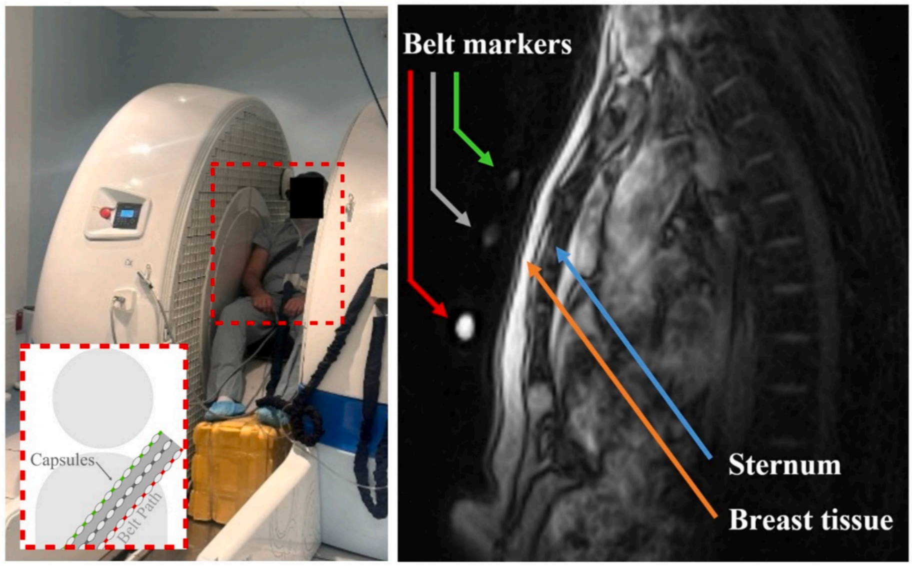

Fig. 1. *Left:* Image of subject seated in MRI machine with shoulder belt with visualization of capsule placement along the belt path. *Right:* Representative resulting imaging of subject upper body in the mid-sagittal plane with visible belt capsules, sternum, and breast tissue.

In a vehicle environment, shoulder belt engagement influences the thorax, upper spine, and head kinematics in a collision, making it a critical factor in injury mitigation (Isaacs et al., 2022). Current available guidance for shoulder belt positioning recommends routing the shoulder belt over the sternum and mid-clavicle (IIHS, 2022). Previous studies have explored the role of diverse occupant anthropometries in introducing variability of this belt positioning. For example, a 350 mm increase of stature has been correlated with a 37 mm outboard shift of the shoulder belt relative to the body midline (Reed et al., 2013). Additionally, obesity was associated with more-inboard shoulder belt positioning and increased slack in the shoulder belt (Reed et al., 2012). Changes in body composition with age, such as a larger waist circumference, have been associated with a higher placement of the shoulder belt on the stomach (Bohman et al., 2019). However, these studies are based largely on gross anthropometric characteristics such as height, weight, and age, leaving much of the variability of subtle body shape characteristics, such as local soft tissue distributions, unanalyzed. The metrics used to define shoulder belt fit also rely on external palpation or landmark estimation, which may confound precise measurement, especially when a substantial amount of superficial soft tissue is present.

Furthermore, there has been limited investigation into the effect of soft tissue across the chest (e.g., breast tissue) on shoulder belt positioning. In belt geometry studies performed via external palpation on volunteers, Jones et al. (2017, 2021) observed an increased gap between the sternum and shoulder belt for females compared to males, as well as a higher placement of the belt relative to the rib cage on females compared to males. This offset, likely due to breast tissue, may be a critical consideration for belt engagement, similar to the effect of increased abdominal soft tissue on lap belt engagement for obese populations (Bohman et al., 2019). However, it is unclear the extent to which soft tissue distribution changes overall shoulder belt routing, and subsequently an individual's ability to appropriately place the belt on the sternum and mid-clavicle.

To better understand how shoulder belts fit and interact with the different torso geometries and tissue distributions, a small preliminary group of five males and five females was scanned in an automotive seat posture using an upright open magnetic resonance (MR) imaging system. This method enabled three-dimensional visualization of the internal body structures and the seat belt routing that was used to quantify the shoulder belt positioning relative to the sternum and clavicle. These measures will aid in the development of occupant injury prediction tools for assessing restraint system robustness accounting for person-to-person variability.

2. Methods

2.1. Volunteer subjects

This study utilized data collected via the methodology described by Booth et al. (2022) and Forman et al. (2024); all procedures were approved by the University of British Columbia's Clinical Research Ethics Board. Ten volunteers (5 male, 5 female) were recruited and gave their informed consent. For measurements and subsequent imaging, volunteers wore study-provided scrubs and their own undergarments. The volunteers were instructed to wear undergarments with no metal (e.g., underwire in a bra, silver threading), to avoid final image distortion. While most of the female subjects wore sports bra-style bras during the experiment, explicit notes were not taken on bra type or fit. No male subjects elected to wear upper body undergarments for the study.

The gross anthropometries for all subjects, including standing height, seated height, weight, BMI, and shoulder width (measured acromion to acromion) were measured (Tale A1). Breast size was calculated as the difference between the chest circumference across the bust and the chest circumference just below the bust. The median of these values for each sex are presented, and the variability of the anthropometric measurements are reported as the bounds of the full and interquartile ranges.

Subjects self-selected an upright position in the driver's seat of a 2016 Acura TLX. Before entering the vehicle, the seat was positioned in the forward-most angle and track position, and the D-ring was set in a neutral location. The subject was prompted to adjust the seating configuration and seat belt to their typical driving position. The horizontal seat base angle was fixed at 12 degrees to match the MRI seat configuration. The seat position along the horizontal track, seatback angle, D-ring location, and head restraint height were recorded. An axis along both the seat base and seat back were created after positioning. Pertinent skeletal landmarks including the suprasternal notch and xiphoid process were measured relative to both axes and the shoulder belt using external palpation. The angle between the shoulder belt and shoulder in the sagittal plane was also recorded.

A non-ferromagnetic replica seat with matched geometry was constructed for safe use in the Upright Open MR imaging (MRI) system (Paramed MROpen EVO, ASG Superconductors, Genoa, Italy; with a gap width of 56 cm). A seat belt made of standard automotive webbing material was marked with continuous lines of vitamin E softgel capsules (400 IU, Nature Made, Pharmavite, San Fernando, California) along the seatbelt top edge, centerline, and bottom edge for visibility in the MR

Table 1

Methods for shoulder belt positioning measurements. All point coordinates and planes were defined using the native MRI coordinate system. (For interpretation of the references to colour in this table, the reader is referred to the web version of this article.)

Belt Routing Measurements	
Sternum-belt distance (SBD)	Distance from the suprasternal notch (top cyan circle) to the intersection of the top edge of the shoulder belt along the sternal midline (green star) in the mid-sagittal plane.
Clavicle-belt horizontal distance (CBH)	Horizontal distance between the projection of the left sternal facet (magenta circle) and the top edge (most medial edge) of the shoulder belt on the YZ plane.
Normalized SBD (SBDn)	SBD divided by the subject's sternal length (Euclidean distance between the suprasternal notch (top cyan circle) and the xiphoid process (bottom cyan circle)).
Normalized CBH (CBHn)	CBH divided by half of the subject's shoulder width (measured on each subject during the initial in-vehicle positioning).
Soft Tissue Measurements	
Top depth: Belt offset at top belt edge	Distance from the shoulder belt top edge at sternal midline intersection point (green star) to the sternum. Measurement taken perpendicular to the sternum angle in the mid-sagittal plane.
Bottom depth: Belt offset at bottom belt edge	Distance from the shoulder belt bottom edge at sternal midline intersection point (red star) to the sternum. Measurement taken perpendicular to the sternum angle in the mid-sagittal plane.
Soft tissue angle	Difference between sternum angle and the shoulder belt angle (line connecting the points in which the belt edges cross the sternal midline in the frontal view) in the mid-sagittal plane. Estimate of soft tissue distribution relative to the sternum.
Schematic	

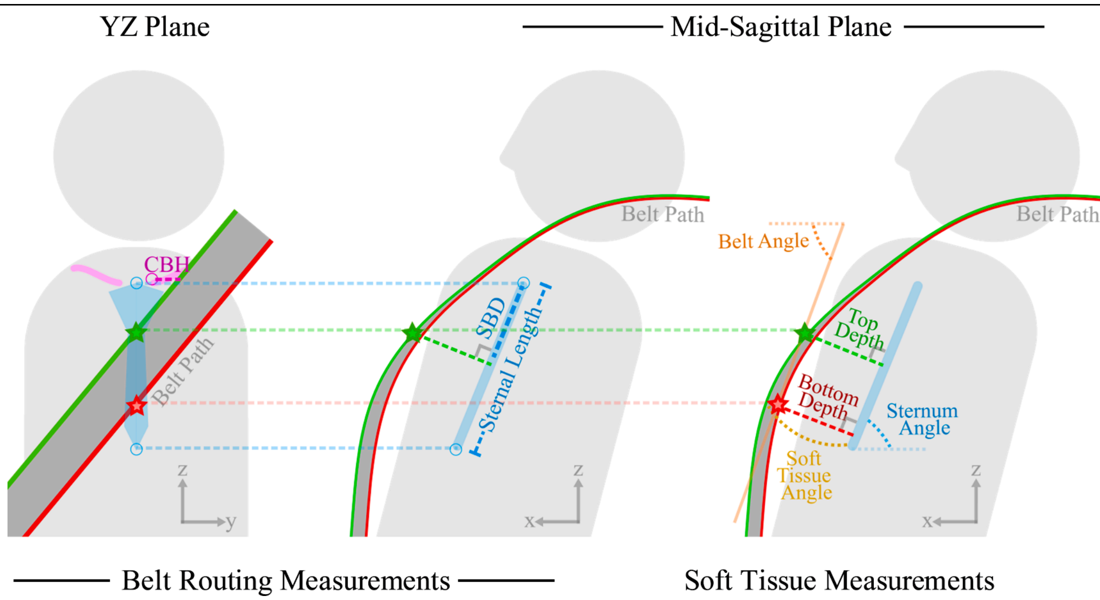

images (Fig. 1). The seat back angle and head restraint height were adjusted to each subject's in-vehicle preferences, and the subjects were positioned using the previously recorded in-vehicle measurements to recreate each individual's preferred automotive posture in the Open MRI scanner. For shoulder belt position matching, the belt distance relative to the suprasternal notch and xiphoid process were replicated from in-vehicle measurements and repeatedly maintained throughout the imaging process. An MR-safe component was attached to the side of the MRI machine that the end of the belt was fed through. The location of this component along the side of the MRI machine was adjusted to replicate the angle in the sagittal plane between the seat belt and the subject's shoulder to that from the in-vehicle environment. After being fed through this component, a 372-gram weight was suspended from the end of the shoulder belt to replicate the tension due to the seat belt retractor. The force of the 372-gram mass under gravity was equivalent to the belt resting tension of a manufacturer seatbelt determined with a handheld belt force gauge. The MR images were captured using a T1-weighted gradient field echo sequence on the sagittal and axial planes. The sequence provided clear visualization of bony landmarks, borders between bone and soft tissue, and the Vitamin E capsules on the belt, while minimizing the scan time for volunteers. Detailed MRI methods, including the T1-weighted sequence parameters, are described in Booth et al. (2022) and Forman et al. (2024).

2.2. Image processing and analysis

Anatomical landmarks were digitized and used to quantify the position, orientation, and shape of the sternum and clavicle using the native MRI coordinate system. Points digitized on the sternum included the suprasternal notch, the inferior-most point on the xiphoid process, and interim points on the lateral borders of the sternal body. Points digitized on the clavicle included the sternal facet at the center of the circular cross section and points along the superficial surface of the shaft. In addition to the skeletal landmarks, each vitamin E capsule along the shoulder belt was digitized, resulting in points every 2–3 cm along the belt edges and centerline. Due to the center of the capsules being digitized, the reported coordinates are offset perpendicular to the belt surface by ½ of the capsule diameter (diameter of 11 mm). Paths of the seat belt's top edge, bottom edge, and centerline were linearly interpolated in three dimensions from the shoulder belt discrete digitized points.

Several measures were investigated to capture the distances between anatomical landmarks and the shoulder belt path (Table 1, Table A2, Fig. A2). The median of these values for each sex are presented, and the variability of the anthropometric measurements are reported as the bounds of the full and interquartile ranges.

Table 2
Summary of age and gross anthropometric metrics of study cohort.

Measure	Group	Median	IQR	Range
Age (years)	Females (n = 5)	34	27–41	24–56
	Males (n = 5)	31	30–52	25–56
Standing Height (cm)	Females (n = 5)	165	163–171	158–179
	Males (n = 5)	182	174–186	155–188
Seated Height (cm)	Females (n = 5)	90	89–91	87–92
	Males(n = 5)	94	91–96	86–97
Weight (kg)	Females (n = 5)	64	63–67	58–74
	Males (n = 5)	95	70–97	58–101
BMI (kg/m^2)	Females (n = 5)	23	22–24	21–28
	Males (n = 5)	27	24–28	23–30
Shoulder Width (cm)	Females (n = 5)	39	39–39	37–41
	Males (n = 5)	44	43–46	43–47
Breast Size (cm)	Females (n = 5)	10	10–11	5–13
	Males (n = 5)	5	5–8	4–9

3. Results

3.1. Volunteer subjects

The male volunteers exhibited greater median standing and seated heights, weights, BMIs, and shoulder widths than the female volunteers in this cohort. Although this volunteer cohort captures a large range of standing heights, representative of much of the national adult population, it is limited to a majority of subjects with BMIs below the national median (Fig. A1) (Fryar et al., 2021). The females of this volunteer subject cohort exhibited similar or lower ranges in all anthropometric measures compared to the male subjects (Table 2).

3.2. Shoulder belt positioning relative to sternum and clavicle

The female subjects in this study exhibited more than three times greater range than the males in the SBD despite lower or similar ranges in all basic anthropometric metrics (Fig. 2, Table 3). Among the female subjects, the top edge of the shoulder belt ranged from one centimeter below the suprasternal notch to halfway down the sternal body, whereas among the male subjects, this edge was positioned within or just below the manubrium for all subjects (Fig. A2). The quantification of the CBH was limited by the visibility of the shoulder belt crossing the clavicle in several scans, resulting in the measure being taken on only six subjects (three males and three females).

3.3. Shoulder belt positioning and soft tissue

The volunteers also exhibited diverse soft tissue distributions and shoulder belt routings across the chest (Fig. 3). For example, for Subject 09 (F) with a soft tissue angle of 12 degrees, substantial offset of the belt from the sternum was observed over the breast tissue in fuller, more distal areas of the breast, and a gap existed between the belt and chest as it crossed the sternal midline (Fig. 3, Bottom Right). Alternatively, minimal soft tissue interaction was observed for Subject 14 (M). This subject had a negative soft tissue angle due to greater displacement of the belt from the sternum near the top of the sternum relative to the bottom (Fig. 3, Top Right). Similar to the SBD and CBH measures, females in this study exhibited larger ranges in the belt offset depths and soft tissue angles compared to the males (Table 4, Fig. 4).

Subjects were also compared to qualitatively illustrate differences in anatomy and shoulder belt routing (Fig. 5, Table 5). Subject pairings were chosen based on similarity in BMI to observe diverse soft tissue distributions within a gross anthropometric group. In an example male and female subject pair (Subject 04 (M) and 05 (F)), the female had a 19-degree greater soft tissue angle than the male (Fig. 5, left). The female in this case had a greater soft tissue distance to the bottom of the belt than the male, while the male subject had a more uniform soft tissue distribution throughout the chest compared to the female.

The variability observed in the female soft tissue angles appeared to be influenced by the observed breast tissue volume and distribution with respect to the sternum. Between an example pair of two female subjects with similar BMIs (Subject 08 (F) and 09 (F)) (Fig. 5, right), a soft tissue angle difference of 20 degrees was measured. Interestingly, subject 08 (F) measured a greater breast size than subject 09 (F), despite having a lower soft tissue angle. However, it is evident that the breast tissue on subject 09 (F) is positioned more medially, causing greater displacement of the shoulder belt as it crosses the sternum.

4. Discussion

The most common external anatomical targets for describing ideal shoulder belt positioning are the sternum and mid-clavicle (IIHS, 2022). The subjects in this study exhibited a wide range of shoulder belt placements relative to these targets. Although the female subjects had

Table 3
Summary of belt routing measurements of study cohort.

Measure	Group	Median	IQR	Range
SBD (mm)	Females (n = 5)	48	41–77	21–116
	Males (n = 5)	58	51–69	51–78
CBH (mm)	Females (n = 3)	13	8–21	2–28
	Males (n = 3)	17	16–17	15–17
SBDn	Females (n = 5)	0.3	0.2–0.4	0.1–0.5
	Males (n = 5)	0.2	0.2–0.2	0.1–0.3
CBHn	Females (n = 3)	0.3	0.2–0.5	0.1–0.7
	Males (n = 3)	0.4	0.4–0.4	0.3–0.4

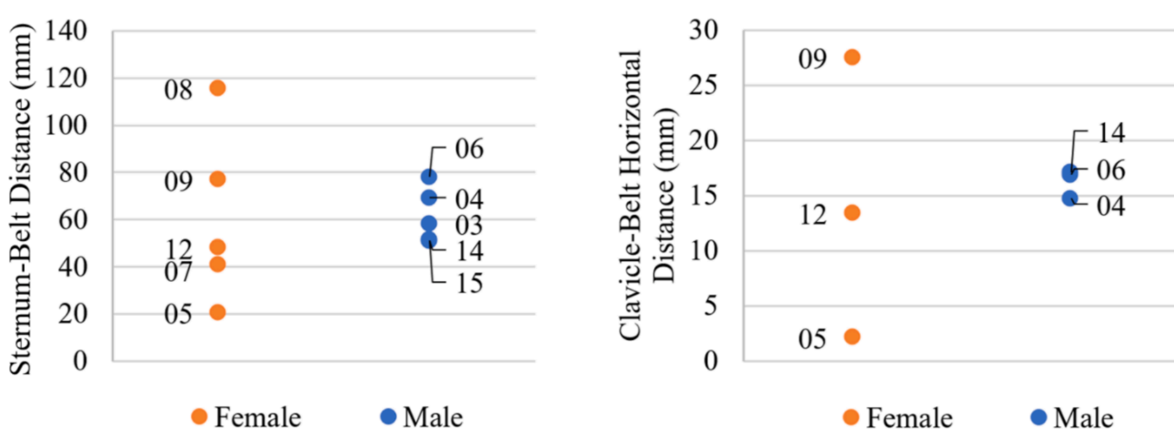

Fig. 2. Plots of the sternum-belt distance (left) and clavicle-belt horizontal distance (right) for females and males. Individual data points are labeled with the associated subject number.

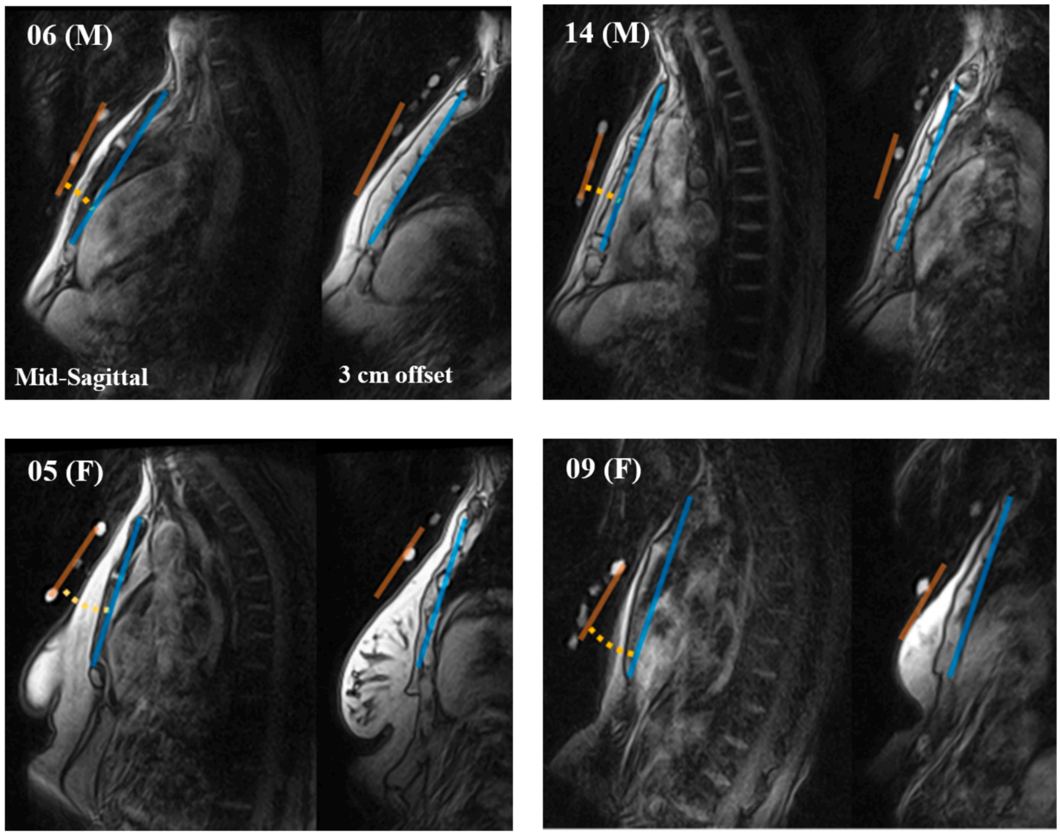

Fig. 3. Example MR images of study subjects with variable soft tissue distribution, with two male subjects on the top and two female subjects on the bottom. The sternum angle and belt angles are represented with blue and orange lines, respectively, and the yellow dashed curve represents the soft tissue angle. For each subject, two MR images are shown: the image on the left displays the mid-sagittal plane, where both soft tissue and belt routing measurements were taken, and the image on the right displays a sagittal plane 3 cm to the left of the mid-sagittal plane to visualize the soft tissue interaction with the belt. (For interpretation of the references to colour in this figure legend, the reader is referred to the web version of this article.)

Table 4
Summary of soft tissue measurements of study cohort.

Measure	Group	Median	IQR	Range
Top Depth (mm)	Females (n = 5)	37	32–37	25–45
	Males (n = 5)	37	35–39	31–43
Bottom Depth (mm)	Females (n = 5)	48	40–52	27–52
	Males (n = 5)	35	32–36	28–47
Soft Tissue Angle (deg)	Females (n = 5)	5	1–12	−8–18
	Males (n = 5)	−1	−3–0	−7–3

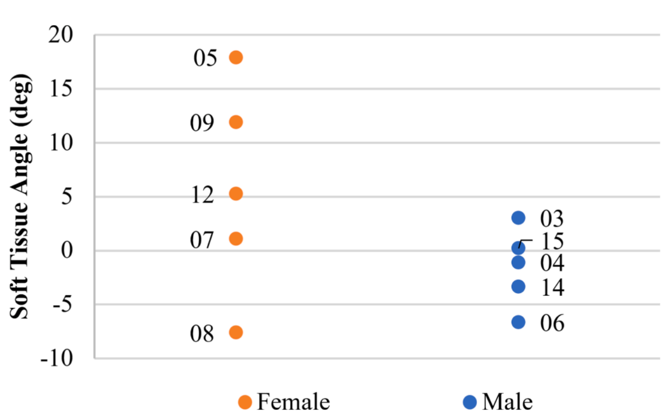

Fig. 4. Plot of the soft tissue angle for females and males. Individual data points are labeled with the associated subject number.

less or similar variability than the males in all gross anthropometric measures, the females exhibited greater ranges in the SBD, CBH, and soft tissue angle compared to the males, which likely indicates an effect of breast tissue on shoulder belt routing.

This study used the soft tissue angle as a simplified metric to quantify shoulder belt displacement from the sternum in the mid-sagittal plane due to soft tissue across the chest. This value varied among subjects of similar BMIs and appeared to be related to the specific local geometry of the breast tissue such as the volume distribution of the soft tissue relative to the sternum. In the subject pair comparisons, the subject with a greater soft tissue angle had a lower SBD, indicating that a greater soft tissue angle may displace the shoulder belt superiorly.

While the soft tissue angle measurement is a step forward in the otherwise understudied role of breast tissue in shoulder belt fit, it overly simplifies breast geometry. Due to this metric being measured at the sternal midline, it does not fully capture the potential effect of breast geometry in more lateral areas with greater soft tissue depths, such as at the breast apex, on the belt routing. It is also evident that a standard breast size measurement, derived from the chest circumference, is not sufficient to identify the anthropometric differences that may cause variable routing patterns. Additional analyses such as shape modeling to quantify breast tissue distributions should be developed for a more comprehensive understanding of this relationship. Potential variables to consider in future analyses include the total volume of each breast, the location of the apex of the breasts on the torso, the location of the breast apices relative to one another, and the curvature of the breasts in the anterior, posterior, medial, and lateral directions from the apex. It is also expected that breast geometries will vary with subject posture, so care should be taken in applying breast geometries from medical imaging (most of which are

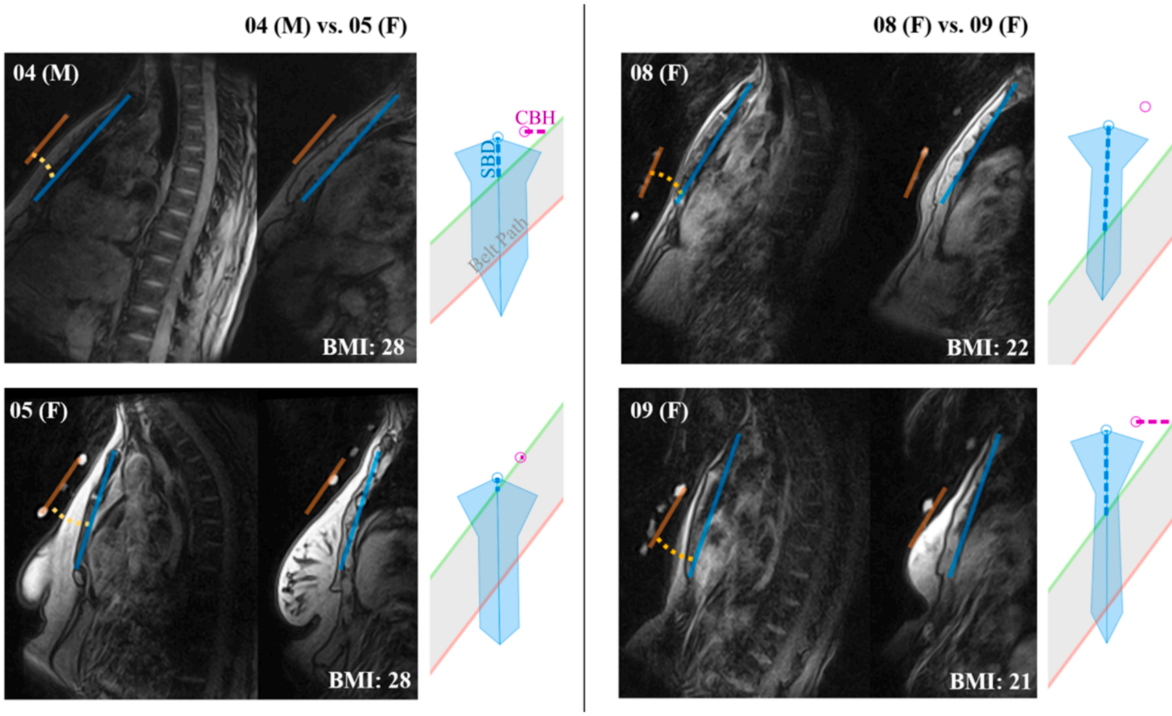

Fig. 5. Comparison of soft tissue angle on subject pairs with similar BMI. Each subject is represented by two MR images in the sagittal view, with the blue and orange lines representing the sternum and shoulder belt angles, respectively, and the yellow dashed curve representing the soft tissue angle. For each subject, the MR image on the left displays the mid-sagittal plane, where both soft tissue and belt routing measurements were taken, and the MR image in the middle displays a sagittal plane 3 cm to the left of the mid-sagittal plane to visualize the soft tissue interaction with the belt. Each subject's YZ plane views are represented on the right by a simplified digitized point reconstruction with the sternum-belt distance (blue dashed line), and clavicle-belt horizontal distance (pink dashed line). No CBH was measured for subject 08 because the point at which the shoulder belt crossed the clavicle was not captured in MR images. (For interpretation of the references to colour in this figure legend, the reader is referred to the web version of this article.)

Table 5
Summary of measurements from pairings in Fig. 5.

Comparison	Subject	BMI	Top Depth (mm)	Bottom Depth (mm)	Soft Tissue Angle (deg)	SBD (mm)	CBH (mm)
Male-Female	04 (M)	28.0	37	36	−1	69	15
	05 (F)	27.9	32	52	18	20	2
Female-Female	08 (F)	21.5	45	*N/A**	−8	116	*N/A***
	09 (F)	20.9	37	52	12	77	28

*Bottom edge of shoulder belt crosses below sternum ** The point at which the shoulder belt crossed the clavicle was not captured in MR images.

obtained in a supine position), to seated or standing postures.

The Open MRI setup used in this study provides a unique opportunity to characterize soft and hard tissue distributions, and their relationships to seat belt paths all in three-dimensions. Due to its non-harmful radiation nature, Open MRI can be used for a broad spectrum of occupant groups with minimal risk. Open MRI can help automotive safety researchers and safety system designers understand seat belt fit in relation to the strong points on the skeleton for a variety of occupant populations and seating configurations (e.g., studying the influence of reclined posture on seatbelt fit; Forman et al. 2024). In this study, Open MRI illustrated the variability of shoulder belt placement relative to the sternum, both from a frontal view (e.g., the location of the shoulder belt as it passes over the sternum) and sagittal view (e.g., belt offset depths and angles). This variability was especially apparent in the female portion of the subject group, where there was more visible diversity in breast tissue volume and distribution.

This study was limited to a small sample size due to cost and available scanner time to execute the imaging. While this volunteer cohort does capture diverse anthropometries, it is not complete. For instance, no subjects with high levels of obesity or breast sizes above 13 cm (associated with a DD cup size) were represented, limiting observation of different routing patterns such as more inboard positioning of the belt across the torso due to obesity, or outboard positioning of the belt on the right breast (Reed et al., 2012). Therefore, observations from this study are preliminary and do not capture the entire population. This method can serve as a tool to supplement or validate techniques such as external palpation that enable data collection with a larger sample size. By compounding investigations of both detailed internal anatomies with high numbers of external geometries, the understanding of important belt routing targets and patterns can continue to be advanced. It is also important to note that this study was predominantly limited to the investigation of sports bra fit. Sports bras provide compression and lack a center gore (the panel in the center of a bra connecting the two cups), limiting the separation of the breasts. Many individuals wear other types of bras regularly. Different bra types offer distinct supports, such lifting or separating the breasts, changing the breast shape and likely affecting the belt path (Suh, 2021). Therefore, future studies should investigate the influence of bras that offer different support (i.e., underwire or a center gore) on the resulting breast geometry and its influence on shoulder belt positioning relative to the sternum and clavicle.

In summary, although understanding differences between sex and anthropometric measures can begin to guide research in vehicle occupant variability, it is also important to acknowledge that within gross demographic categories, variability is still abundant. Factors determining subject positioning within a vehicle environment, specifically in relation to the shoulder belt, cannot be simplified to a single gross descriptor of anthropometry. Shoulder belt positioning depends on a combination of subject factors, from broad measures like height and weight, to subtle complexities like soft tissue distribution. By understanding the variability introduced in seatbelt fit due to diverse anthropometries, we are better prepared to both evaluate the ability of current occupant models to capture these effects of anthropometry on seatbelt fit, as well as further incorporate dimensions of person-to-person variability into such models. Additionally, integrating the belt routing metrics studied here into computational crash test studies can be used to assess how a pretensioner may mitigate some of these differences in initial belt placement and skeletal proximity that result from differences in anthropometry. Such models may then be used to investigate the down-stream implications on restraint interaction and injury risk. We recommend future work investigate the effects of more subtle body shape variability, such as local soft tissue distributions, on restraint interaction using human body modeling, including critically reviewing (and potentially refining) the biofidelity of the superficial soft tissue acting as an intermediary between the belt system and the underlying skeleton.

CRediT authorship contribution statement

Olivia Mergler: Writing – review & editing, Writing – original draft, Visualization, Methodology, Investigation, Formal analysis, Data curation, Conceptualization. **Corina Espelien:** Writing – review & editing, Writing – original draft, Supervision, Investigation, Formal analysis, Conceptualization. **Gabrielle R. Booth:** Writing – review & editing, Resources, Methodology, Data curation. **Carolyn Roberts:** Writing – review & editing, Methodology, Data curation, Conceptualization. **Paris Vakiel:** Writing – review & editing, Data curation. **Sarah Romani:** Writing – review & editing, Data curation. **Honglin Zhang:** Writing – review & editing, Resources, Data curation. **Bengt Pipkorn:** Writing – review & editing, Conceptualization. **Gunter P. Siegmund:** Writing – review & editing, Methodology, Conceptualization. **Peter A. Cripton:** Writing – review & editing, Funding acquisition, Conceptualization. **Jason Forman:** Writing – review & editing, Supervision, Methodology, Investigation, Funding acquisition, Formal analysis, Conceptualization.

Funding

Autoliv Research.

Declaration of competing interest

The authors declare that they have no known competing financial interests or personal relationships that could have appeared to influence the work reported in this paper.

Acknowledgements

The authors would like to thank Autoliv Research for providing financial support for this study. We are also grateful for the volunteers who participated in this study. Their cooperation has been instrumental in advancing our understanding of automobile safety among diverse populations.

Appendix

Table A1
Subject age and gross anthropometries.

		Age and Gross Anthropometries							
	Sub.	Age (yrs)	Standing Height (cm)	Seated Height (cm)	Weight (kg)	BMI (km/m^2)	Shoulder Width (cm)	Breast Size (cm)	Seatback Angle (deg)
Female	05	24	163	89	74	28	37	11	10
	07	27	165	90	64	24	39	10	20
	08	34	171	92	63	22	41	13	20
	09	41	179	91	67	21	39	5	16
	12	56	158	87	58	23	39	10	10
Male	03	25	182	96	101	30	46	9	20
	04	31	186	94	97	28	44	8	20
	06	30	174	91	70	23	43	5	20
	14	52	155	86	58	24	43	5	10
	15	56	188	97	95	27	47	4	20

Table A2
Subject belt routing and soft tissue measurements.

		Belt Routing				Soft Tissue		
	Sub.	SBD (mm)	CBH (mm)	SBDn	CBHn	Top Depth (mm)	Bottom Depth (mm)	Soft Tissue Angle (deg)
Female	05	21	2	0.1	0.1	32	52	18
	07	41	N/A*	0.2	N/A*	25	27	1
	08	116	N/A*	0.5	N/A*	45	N/A**	−8
	09	77	28	0.4	0.7	37	52	12
	12	48	13	0.3	0.3	37	44	5
Male	03	58	N/A*	0.2	N/A*	43	47	3
	04	69	15	0.2	0.3	37	36	−1
	06	78	17	0.2	0.4	39	32	−7
	14	51	17	0.3	0.4	31	28	−3
	15	51	N/A*	0.1	N/A*	35	35	0

*Bottom edge of shoulder belt crosses below sternum
**The point at which the shoulder belt crossed the clavicle was not captured in MR images.

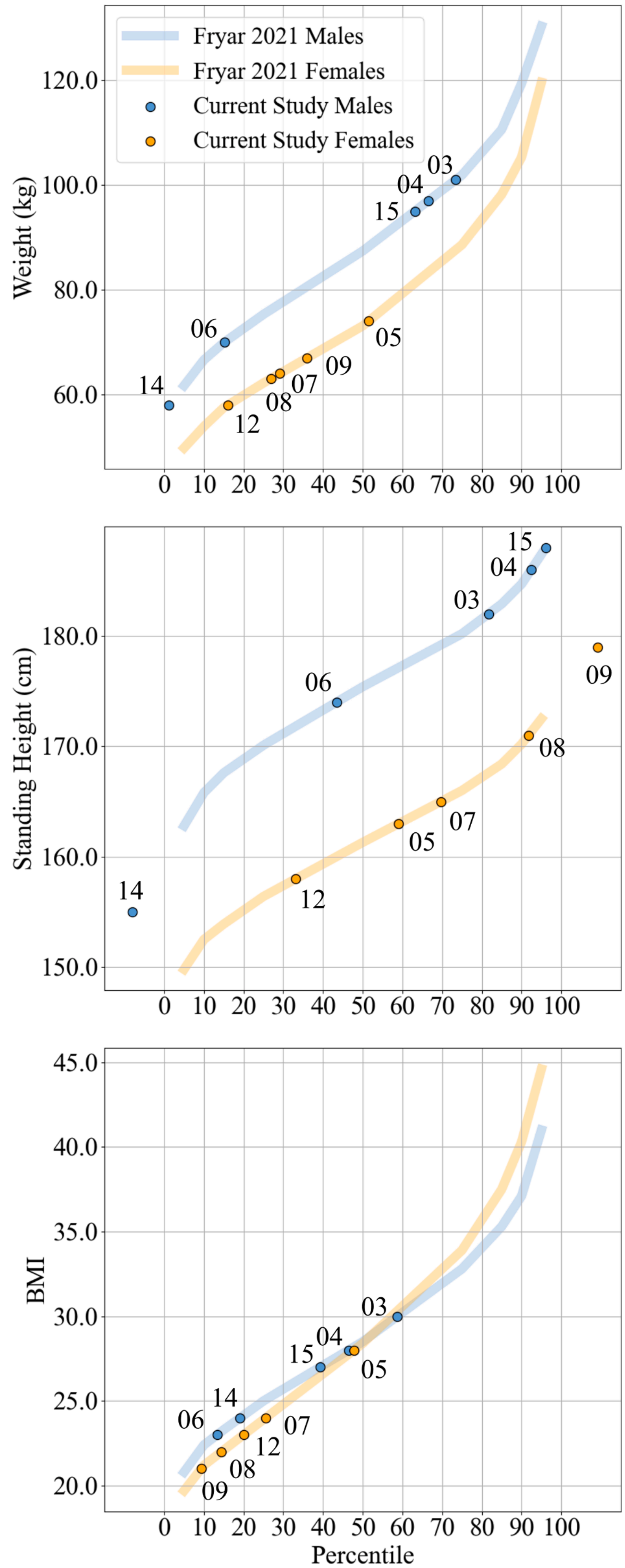

Fig. A1. Plot of the weights, standing heights, and BMIs versus the associated percentile for the US adult population from Fryar et al. (2021). The curves represent the distribution of US adults, while the points represent the anthropometric measures within this study cohort. Data points are labeled with the associated subject number.

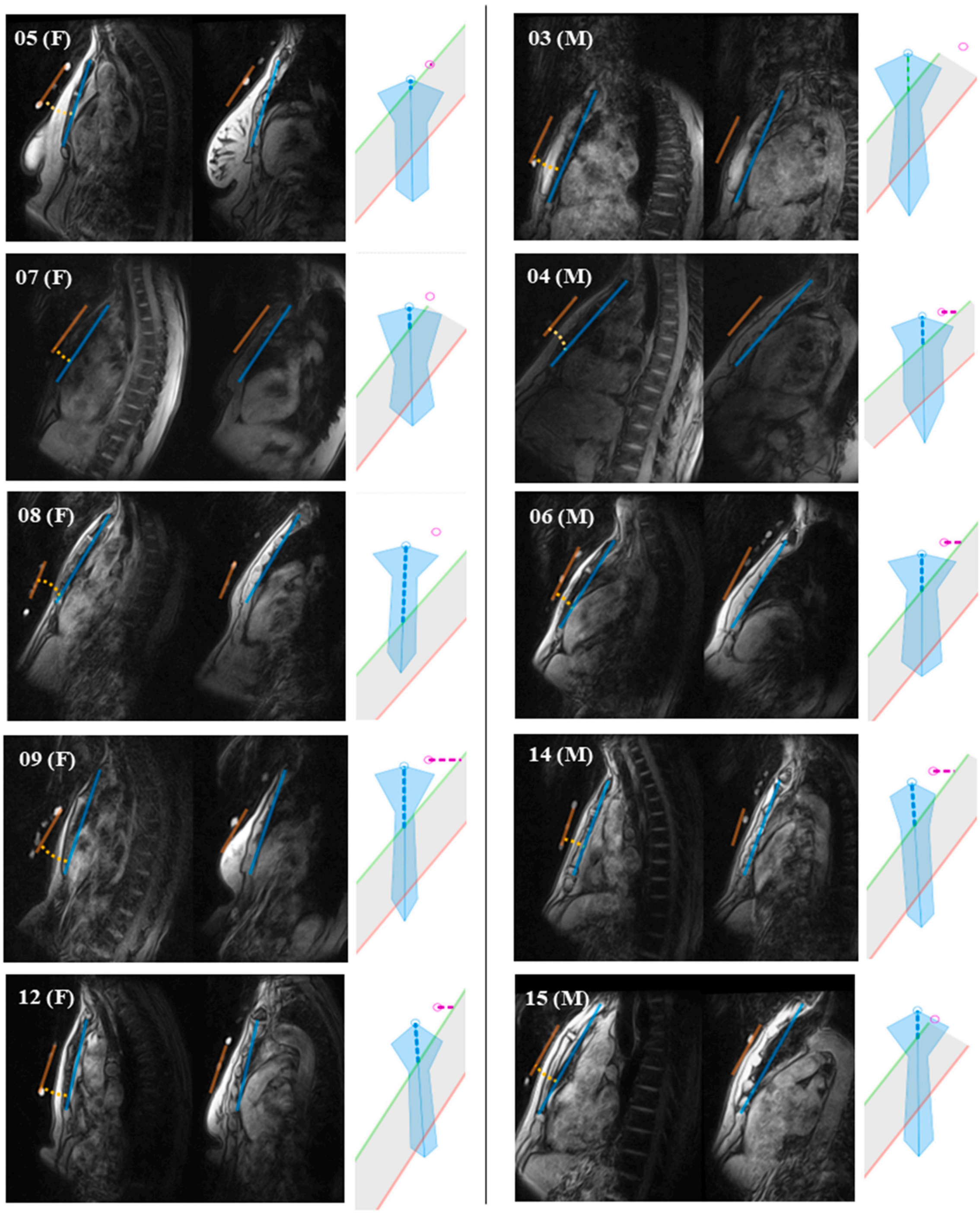

Fig. A2. Each subject is represented by an MR image in the sagittal view, with the blue and orange lines representing the sternum and shoulder belt angles, respectively, and the yellow dashed curve representing the soft tissue angle. For each subject, the MR image on the left displays the mid-sagittal plane, where both soft tissue and belt routing measurements were taken, and the image in the middle displays a sagittal plane 3 cm to the left of the mid-sagittal plane to visualize the soft tissue interaction with the belt. Each subject's YZ plane views are represented on the right by a simplified digitized point reconstruction with the SBD (blue dashed line), and CBH (pink dashed line). (For interpretation of the references to colour in this figure legend, the reader is referred to the web version of this article.)

References

Bohman, K., Osvalder, A.-L., Ankartoft, R., Alfredsson, S., 2019. A comparison of seat belt fit and comfort experience between older adults and younger front seat passengers in cars. Traffic Injury Prevention 20, S7–S12. https://doi.org/10.1080/15389588.2019.1639159.

Booth, G.R., Roberts, C.W., Romani, S., Mergler, O., Zhang, H., Pipkorn, B., Siegmund, G. P., Cripton, P.A., Forman, J., 2022. Methodology to measure seat belt fit in relation to skeletal geometry using an upright open MRI. Traffic Inj Prev 23, S199–S201. https://doi.org/10.1080/15389588.2022.2124805.

Boulanger, B.R., Milzman, D., Mitchell, K., Rodriguez, A., 1992. Body habitus as a predictor of injury pattern after blunt trauma. J Trauma 33, 228–232. https://doi.org/10.1097/00005373-199208000-00011.

Brumbelow, M.L., Jermakian, J.S., 2022. Injury risks and crashworthiness benefits for females and males: Which differences are physiological? Traffic Inj Prev 23, 11–16. https://doi.org/10.1080/15389588.2021.2004312.

Forman, J., Booth, G., Mergler, O., Romani, S., Zhang, H., Roberts, C., Siegmund, G.P., Pipkorn, B., Cripton, P., 2024. Variability in Body Shape, Superficial Soft Tissue

Geometry, and Seatbelt Fit Relative to the Pelvis in Automotive Postures—Methods for Volunteer Data Collection With Open Magnetic Resonance Imaging. Journal of Biomechanical Engineering 146. https://doi.org/10.1115/1.4064477.

Forman, J., Poplin, G.S., Shaw, C.G., McMurry, T.L., Schmidt, K., Ash, J., Sunnevang, C., 2019. Automobile injury trends in the contemporary fleet: Belted occupants in frontal collisions. Traffic Injury Prevention 20, 607–612. https://doi.org/10.1080/15389588.2019.1630825.

Fryar, C.D., Carroll, M.D., Gu, Q., Afful, J., Ogden, C.L., 2021. Anthropometric reference data for children and adults : United States, 2015-2018.

Gepner, B., Joodaki, H., Sun, Z., Jayathirtha, M., Kim, T., Forman, J., Kerrigan, J., 2018. Performance of the Obese GHBMC Models in the Sled and Belt Pull Test Conditions. In: IRC-18-60. Presented at the International Research Council on the Biomechanics of Injury, Athens, Greece.

Hanna, R., Hershman, L., 2009. Evaluation of Thoracic Injuries Among Older Motor Vehicle Occupants (No DOT HS 811 101). Mathematical Analysis Division, National Center for Statistics and Analysis.

IIHS, 2022. Dummy Seating Procedure for Rear Outboard Positions: Version II.

Isaacs, J.L., George, J., Campolettano, E., Cutcliffe, H., Miller, B., 2022. The Role of Three-Point Restraints for Occupants in Moderate Severity Frontal Collisions (SAE Technical Paper No. 2022- 01–0845). SAE International, Warrendale, PA. doi: 10.4271/2022-01-0845.

Jones, M., Ebert, S., Hu, J., Reed, M., 2017. Effects of High Levels of Obesity on Lap and Shoulder Belt Paths.

Jones, M.L.H., Buckley, L., Ebert, S.M., Reed, M.P., Hallman, J.J., 2018. Evaluating an intervention to improve belt fit for adult occupants. Journal of Safety Research 64, 93–104. https://doi.org/10.1016/j.jsr.2017.12.013.

Jones, M.L.H., Ebert, S.M., Varban, O., Hu, J., Reed, M.P., Weerappuli, P., Sundarajan, S., Barbat, S., 2021. Effect of Class I–III obesity on driver seat belt fit. Traffic Injury Prevention 22, 547–552. https://doi.org/10.1080/15389588.2021.1945590.

Kent, R., Lee, S.-H., Darvish, K., Wang, S., Poster, C.S., Lange, A.W., Brede, C., Lange, D., Matsuoka, F., 2005. Structural and material changes in the aging thorax and their role in crash protection for older occupants. Stapp Car Crash J 49, 231–249. https://doi.org/10.4271/2005-22-0011.

Suh, M., 2021. Breast Size and Anthropometric Changes through Brassieres. Journal of Textile & Apparel Technology & Management (JTATM) 12, 1–15.

Reed, M.P., Ebert, S.M., Hallman, J.J., 2013. Effects of driver characteristics on seat belt fit. Stapp Car Crash J 57, 43–57. https://doi.org/10.4271/2013-22-0002.

Reed, M.P., Ebert-Hamilton, S.M., Rupp, J.D., 2012. Effects of Obesity on Seat Belt Fit. Traffic Injury Prevention.